Clays and Clay Minerals, Vol. 69, No. 5:576–588, 2021

GENTAMICIN-MONTMORILLONITE INTERCALATION COMPOUNDS AS AN ACTIVE COMPONENT OF HYDROXYPROPYLMETHYLCELLULOSE BIONANOCOMPOSITE FILMS WITH ANTIMICROBIAL PROPERTIES

Margarita Darder[1], Jing He[1,2], Laurent Charlet[2], Eduardo Ruiz-Hitzky[1], and Pilar Aranda[1]*

[1]Instituto de Ciencia de Materiales de Madrid, CSIC, Madrid, Spain
[2]Université Joseph Fourier, Grenoble, France

Abstract—The present study introduces an overview of gentamicin-clay mineral systems for applications in biomedicine and then focuses on the development of a series of gentamicin/clay hybrid materials to be used as the bioactive phase of hydroxypropylmethylcellulose (HPMC) to produce bionanocomposite membranes possessing antimicrobial activity of interest in wound-dressing applications. Gentamicin (Gt) was adsorbed from aqueous solutions into a montmorillonite (Cloisite®-Na^+) to produce intercalation compounds with tunable content of the antibiotic. The hybrids were characterized by CHN chemical analysis, energy-dispersive X-ray analysis, X-ray diffraction, Fourier-transform infrared spectroscopy, and thermogravimetric analysis, confirming the intercalation of Gt by an ion-exchange mechanism. The release of Gt from the hybrids was tested in water and in buffer solution to check their stability. Hybrids with various amounts of Gt were incorporated into a HPMC matrix at various loadings and processed as films by the casting method. The resulting Gt-clay/HPMC bionanocomposites were characterized by means of field-emission scanning electron microscopy, and were also evaluated for their water-adsorption and mechanical properties to confirm their suitability for wound-dressing applications. The antimicrobial activity of the bionanocomposite films was tested in vitro toward various microorganisms (*Escherichia coli, Pseudomonas aeruginosa, Staphylococcus aureus,* methicillin-resistant *Staphylococcus aureus* (MRSA), vancomycin-resistant *Enterococcus faecium, Acinetobacter baumannii*, and *Klebsiella pneumonia*), showing a complete bacterial reduction even in films with small Gt contents.

Keywords—Antibacterial activity · Bionanocomposite films · Gentamicin · Hydroxypropylmethyl cellulose · Montmorillonite · Wound dressing

INTRODUCTION

The use of clays in health care has been known by humans since ancient times, probably because they are abundant in nature and have been used for a long time for various purposes, from pottery to early writing, including hybrid and composite materials (Faustini et al., 2018). In this way, raw clays found in soils and muds have been useful in the treatment of infections, as de-toxin agents, antidotes of poisons, or topical dermatologic treatments (Rautureau et al., 2017; Finkelman, 2019; Williams, 2019). Clays can be used directly, e.g. to remove toxins and poisons, in geophagy (Allègre, 2012), or as treatment of specific skin diseases, such as Burili ulcers (Williams & Haydel, 2010; Williams, 2017) or, more recently, employed as carriers of specific agents, typically of drugs (Viseras et al., 2010; Oh et al., 2012; Yang et al., 2016; Ruiz-Hitzky et al., 2019; Stavitskaya et al., 2019; Viseras et al., 2019) but also of other agents such as DNA (Choy et al., 2000; Castro-Smirnov et al., 2016, 2017) or viruses (Ruiz-Hitzky et al., 2009; Wicklein et al., 2012, 2016), for treatment of diverse diseases.

Clays involved in biomedical and pharmaceutical applications include layered 1:1 and 2:1 phyllosilicates, typically kaolinite and smectites, fibrous and tubular clays, such as sepiolite and halloysite nanotubes, as well as certain layered double hydroxides (LDH). Commonly, the final therapeutic system is associated with other components to reach an improved efficiency and a controlled release of the active principle, though its design is determined by the final application. The route of administration can be oral, transdermal, or other to achieve a local release, targeting organs or cells, such as the eyes, the cheek, the vagina, bones, or blood vessels (Kim et al., 2016). The components involved were selected to introduce biocompatibility, to improve solubility and/or adsorption of the drug or muco-adhesive, and/or to target certain properties, including sustained and/or controlled release. Very often, these components are biocompatible and biodegradable polymers and biopolymers, the role of which often is to protect the drug-clay system providing a sustained release (Park et al., 2008), but, also, they are used increasingly to produce a controlled or even targeted release of a drug (Ribeiro et al., 2014; Rebitski et al., 2020).

Antibiotics are among the diverse types of drugs the release of which has been explored in combination with clays. In general, the association with clay improves the antibiotic stability in the medium and affords a sustained release, which is crucial for certain types of applications, e.g. in wound dressing or tissue engineering. One of the antibiotic species that has attracted most interest is gentamicin (Gt). This antibiotic is an

This paper belongs to a special issue on 'Clay Minerals in Health Applications'

* E-mail address of corresponding author: pilar.aranda@csic.es
DOI: 10.1007/s42860-021-00156-3

aminoglycoside species produced by fermentation of *Micromonospora purpurea* that consists of a mixture of basic, water-soluble compounds containing the aminocyclitol 2-deoxystreptamine and two additional amino sugars (MacNeil & Cuerpo, 1995). The Gt formula (Fig. 1a) shares many structural and functional features with other antibiotics containing streptamine or its derivatives, such as streptomycin, neomycin, and kanamycin (Butko et al., 1990), and has been used to treat many types of bacterial infections, particularly those caused by Gram-negative organisms (Moulds & Jeyasingham, 2010). Although application of Gt in human medicine has declined, its use in veterinary medicine and agriculture is still intense, and it could be relevant in the treatment of certain topical injuries or for avoiding internal infection caused by diverse types of implants.

Gentamicin has been associated with several layered silicates from kaolinite (Hui et al., 2019) to smectites (Rapacz-Kmita et al., 2015, 2017a, 2017b; Iannuccelli et al., 2018; Jeong et al., 2018), and has also been incorporated in halloysite nanotubes (Rapacz-Kmita et al., 2019) and layered double hydroxides (Carja et al., 2007). Most of these studies analyzed the release of the antibiotic from the support and provided results on their antibacterial properties against various pathogens such as *E. coli*, *S. aureus,* or *S. epidermidis*. Very few of the studies, however, carried out a proper and accurate characterization of the Gt-clay compounds. The most systematic and complete study was probably that by Iannuccelli et al. (2018) which reported the adsorption of Gt in a natural bentonite from Iglesias (Sardinia, Italy) before and after purification and activation with Na^+ ions. The raw mineral adsorbed more Gt and so was the first to be used in the present study. Those authors claimed the possible intercalation of Gt and carried out simulations on the possible arrangement of the molecule as a monolayer in the interlayer region although XRD patterns were not shown. The adsorption was driven by an ion-exchange reaction and the presence of S suggested the incorporation of a certain amount as Gt sulfate. Interestingly, the study showed the incorporation of the system into petroleum jelly and application on the skin (in vivo experiment with three volunteers) revealed that the association of the antibiotic with the clay allowed a sustained release and so a more effective anti-infective therapy.

The combination of Gt-clay systems and biocompatible polymers, in particular biopolymers, has been explored with various biomedical purposes mainly addressing the preparation of bioactive coatings for application in implants and scaffolds with the intention of reducing infections. Thus, for instance, Gt was included in the lumen of halloysite nanotubes that were then combined with methyl methacrylate to produce efficient halloysite/poly(methyl methacrylate) bone-cement composites provided with prophylactic activity (Wei et al., 2012). Typical approaches applied to produce coatings of potential relevance in implant applications included Layer-by-Layer (LbL) and spray-drying techniques. Thus, the production of multilayer films by LbL may involve the assembly of a layer of the clay, e.g. montmorillonite, and then one of an organic component, e.g. hyaluronic acid (Wang et al., 2018) or poly-L-lysine (Xu et al., 2017), in which Gt is embedded on the top of substrates such as glass discs, polydimethylsiloxane (PDMS), or silicon wafers. The presence of the antibiotic in the grown coating acted as a biofilm inhibitor as it was released slowly. Gentamicin could also be loaded once the LbL structure is produced as reported for montmorillonite/polyacrylic acid (PAA) systems in which the swelling properties afforded by PAA and the number of grown multilayers are used to control the amount of Gt entrapped and released (Pavlukhina et al., 2014). The creation of multilayered coatings proved especially useful as the presence of the clay layers provided an effective barrier, making it possible to tune and stage release of the antibiotic (Min et al., 2014). Electro-spraying is an alternative methodology applied to produce coatings of montmorillonite/chitosan composite nanospheres in which an antibiotic (e.g. Gt, vancomycin) is included to provide sustained, in situ delivery at implanted bone sites (Kimna et al., 2019). The related electrospinning technique has been explored recently to produce nanoarchitectured composite membranes based on the formation of poly(ε-caprolatone)/montmorillonite fibers in which Gt was also incorporated in order to produce scaffolds provided with bactericide properties for wound healing, tissue-engineering, and other applications (Reshmi et al., 2018). Other types of processing included the direct solvent-casting preparation of films from dispersions of the polymer incorporating the clay-antibiotic component as reported by Rapacz-Kmita et al. (2020) for developing biodegradable poly(lactic acid)-montmorillonite nanocomposites with antibacterial properties. Electrospinning can be also applied to produce multilayered membranes of poly(lactic acid) reinforced with halloysite, which are later loaded with Gt to produce bioactive films for bone-regeneration applications (Pierchala et al., 2018). The association of Gt with the clay and further combination with water-soluble polymers allowed the production of hydrogels, e.g. poly(vinyl alcohol)/montmorillonite-Gt (Sirousazar, 2013) or chitosan/halloysite-Gt (Luo & Mills, 2019), that can be further conformed, e.g. as films or beads, and submitted to freeze-drying to produce drug-delivery systems for diverse biomedical applications, including wound dressings.

Burn-wound infections are among the most important and potentially serious complications that occur during the acute period following injury. Systemic treatment against infection is limited by inadequate wound perfusion, which restricts migration of host immune cells and the delivery of antimicrobial agents to the wound. In this case, the local concentration of the antibiotics may be insufficient and may lead to bacterial resistance (Elsner et al., 2011). The widespread application of a topical antimicrobial agent on the open burn-wound surface can reduce substantially the microbial load and risk of infection (Murphy et al., 2003). The typical burn wound is colonized initially predominantly by Gram-positive organisms, which are replaced by antibiotic-susceptible Gram-negative organisms within 1 week of the burn injury. Gentamicin is used to treat many types of bacterial infections, particularly those caused by Gram-negative organisms and it can protect the recovering tissue from potential infection or re-infection and therefore

https://doi.org/10.1007/s42860-021-00156-3 Published online by Cambridge University Press

has been used to cure burn wounds (Moulds & Jeyasingham, 2010). Gentamicin-eluting collagen sponges have been found useful in both partial-thickness and full-thickness burn wounds (Elsner et al., 2011). A new concept of wound dressing, which is based on a polyglyconate mesh coated with a porous poly-(DL-lactic-*co*-glycolic acid) matrix loaded with Gt, is applied to burn wounds (Aviv et al., 2007; Elsner et al., 2011).

Within this general context, the present contribution addresses a systematic study on the adsorption of Gt to montmorillonite and the further incorporation of some of the intercalation compounds produced into hydroxypropylmethylcellulose (HPMC) to produce bionanocomposite films for wound-dressing applications. HPMC (Fig. 1b) has been selected because of its properties as a hydrophilic carrier material including applications in oral drug-delivery systems (Colombo, 1993). The incorporation of the Gt-clay mineral component as a reinforcing and active nanofiller is expected to lead to HPMC bionanocomposite films of the necessary mechanical strength, while the combined binding matrix is aimed at providing adequate moisture control and release of antibiotics to protect the wound bed from infection and promote healing. Mechanical properties, moisture-adsorption behavior and the antimicrobial activity of bionanocomposite films of various compositions were also examined with a view to establishing their appropriateness for potential application as wound-dressing tissues.

EXPERIMENTAL

Materials and Reagents

Gentamicin sulfate from *Micromonospora purpurea* was supplied by Sigma-Aldrich (Tres Cantos, Spain). The montmorillonite commercialized as Cloisite® Na^+ Nanoclay, with a cationic exchange capacity of 92.6 meq/100 g, was obtained from Southern Clay Products (Rockwood Additives, Gonzales, Texas, USA) and used in this study without further purification. The polysaccharide hydroxypropylmethylcellulose (HPMC; ~22 kDa; viscosity 40–60 cP, 2% in H_2O, 20°C, methoxyl content: 28–20%, hydroxypropoxyl content: 7–12%), sodium phosphate monobasic monohydrate (ACS reagent, ≥98%), and phthaldialdehyde solution reagent (P0532), which contains phthaldialdehyde (1 mg/mL), Brij® 35, methanol, 2-mercaptoethanol, potassium hydroxide, and boric acid, pH 10.4, were obtained from Sigma-Aldrich (Tres Cantos, Spain). Deionized water (resistance of 18.2 MΩ cm) was obtained with a Maxima Ultra Pure Water system from Elga (Celle, Germany).

Preparation of Gentamicin-montmorillonite Hybrids

A series of Gt sulfate solutions was prepared by dissolving certain amounts of Gt sulfate into deionized water in order to obtain concentrations ranging from 25 to 7300 mg/L, as detailed in Table 1. 50 mg of montmorillonite was added to 5 mL of each Gt solution, reaching a final clay content of 1 wt.%. Thus, the starting amounts of Gt per 1 g of clay to prepare a set of six samples were between 25 and 730 mg/g, as summarized in Table 1. The Gt-montmorillonite (Gt-Mnt) mixtures in air-tight bottles covered by aluminum film were shaken for 7 days under constant temperature (21°C), and then centrifuged at the end of the adsorption process to remove the supernatants. The Gt-Mnt hybrids obtained were air-dried at 40°C under dark conditions.

Preparation of HPMC/gentamicin-montmorillonite Bionanocomposite Films

The HPMC bionanocomposite films were prepared by incorporation of the freshly prepared hybrid labeled as Gt-Mnt-500, obtained from a starting amount of 500 mg of\ Gt per g of montmorillonite, in the HPMC solution obtained by dissolving 2 g of HPMC in 100 mL of distilled water. To study the effect of the Gt-Mnt hybrid loading in the HPMC film

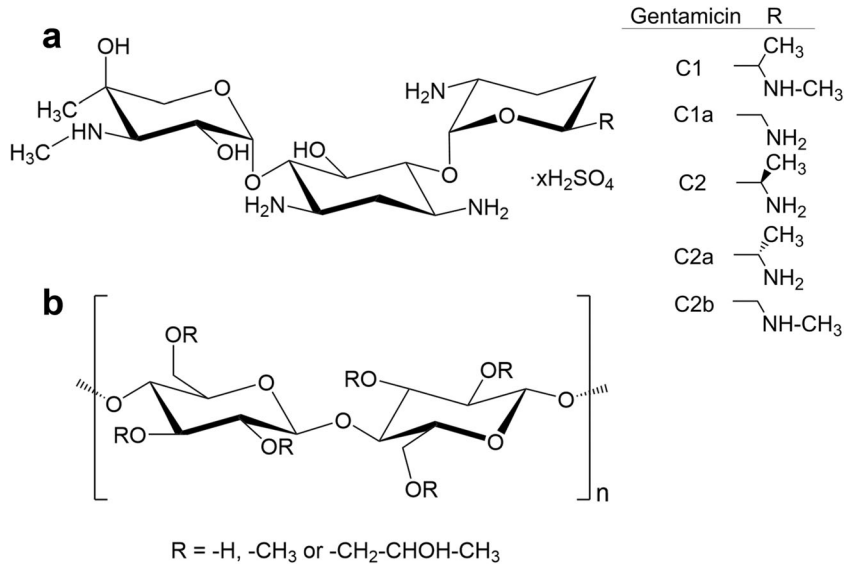

Fig. 1. Chemical structures of **a** the major components of Gt sulfate and **b** the polysaccharide hydroxypropylmethylcellulose (HPMC)

https://doi.org/10.1007/s42860-021-00156-3 Published online by Cambridge University Press

Table 1. Samples prepared for the adsorption isotherm experiment

Sample code	Gentamicin concentration (mg/L)	Mass of gentamicin (mg)	Starting amount of gentamicin (mg) per g of clay
Gt-Mnt-25	250	1.25	25
Gt-Mnt-50	500	2.5	50
Gt-Mnt-200	2000	10	200
Gt-Mnt-500	5000	25	500
Gt-Mnt-600	6000	30	600
Gt-Mnt-730	7300	36.5	730

matrix, various amounts of nanohybrid were added to 10 mL of the 2% w/v HPMC solution to obtain various film compositions as indicated in Table 2. The mixtures of HPMC solution and different amounts of Gt-Mnt-500 hybrid were homogenized by stirring at 400 rpm at 40°C for 4 h, and then dropped onto plastic plates (100 mm×100 mm) and placed in a laminar flow hood provided with a UV lamp. The samples were sterilized by UV irradiation for 15 min, and then the films were formed by solvent evaporation for 4 days.

Characterization

The amount of organic matter in the Gt-Mnt samples was determined by CHN elemental chemical microanalysis using a Perkin-Elmer 2400 analyzer (Waltham, Massachusetts, USA). Powder X-ray diffraction (XRD) patterns of pristine montmorillonite and the antibiotic-loaded hybrids were obtained using a Bruker D8 Advance diffractometer (Billerica, Massachusetts, USA) with CuKα radiation and a scan speed of 0.02°/s. The thermal behaviors of the various materials were analyzed from the simultaneously recorded thermogravimetric (TG) and differential thermal analysis (DTA) curves (using a Seiko (Chiba, Japan) SSC/5200 instrument in experiments carried out under air atmosphere (flux of 100 mL min^{-1}) from room temperature to 1000°C at a heating rate of 10°C min^{-1}). Fourier-transform infrared (FTIR) spectra were measured in transmission absorption mode on a Bruker (Billerica, Massachusetts, USA) IFS 66v/S spectrophotometer, with samples prepared in KBr pellets, throughout the 4000–250 cm^{-1} region. The surface and cross-sections of the films were observed directly using a Field Emission-Scanning Electron Microscope FEI NOVA NanoSEM 230 (Eindhoven, Netherlands) without no conducting coating required. Moisture sorption was investigated using an Aquadyne DVS dynamic water vapor sorption analyzer from Quantachrome Instruments (Boynton Beach, Florida, USA). Moisture-sorption isotherms were recorded at 25 ± 0.3°C in the range of relative humidity from 0 to 95% by using ~7 mg of sample.

Mechanical Properties

Films used for tensile tests were conditioned at ~65% RH at 15°C prior to the measurements. A Model 3345 Instron Universal Testing Machine (Instron Engineering Corporation, Canton, Massachusetts, USA) was used to determine the maximum percentage elongation at break (%), and elastic modulus E (or Young's modulus) according to ASTM standard method D 882-88. The sample films with a rectangular shape (~60 mm×15 mm) were mounted between the grips with an initial separation of ~25 mm. The cross-head speed was set at 5 mm min^{-1}. Three replicates were run for each film sample.

In vitro Gentamicin Release from the Gentamicin-montmorillonite Hybrids

The amount of Gt released was detected in the supernatant by UV-Vis spectrophotometry after reaction with phthaldialdehyde. For this purpose, a weighed amount of Gt-Mnt-600 (~60 mg) was added to 5 mL of bidistilled water, kept under shaking at room temperature for various time intervals, and then the samples were centrifuged (15 min, 10,000 rpm, 14,087×*g*) in order to obtain the supernatants. The determination procedure consisted of mixing 1 mL of the supernatant

Table 2. Composition of the prepared HPMC/Gt-montmorillonite bionanocomposite films using the Gt-Mnt-500 hybrid

Sample label	Hybrid content (%)	Clay content (%)	Gentamicin content (%)
6.0%Gt-Mnt-HPMC	62.4	56.4	6.0
3.4%Gt-Mnt-HPMC	35.6	32.2	3.4
2.1%Gt-Mnt-HPMC	21.7	19.6	2.1
1.4%Gt-Mnt-HPMC	14.2	12.9	1.4
0.5%Gt-Mnt-HPMC	5.2	4.7	0.50
0.26%Gt-Mnt-HPMC	2.7	2.4	0.26
HPMC	0	0	0
Mnt-HPMC	0	60	0

https://doi.org/10.1007/s42860-021-00156-3 Published online by Cambridge University Press

with 1 mL of phthaldialdehyde solution reagent and 2 μl of 2-mercaptoethanol. The mixtures were allowed to stand for 30 min at room temperature, and then the absorbance was measured between 450 and 320 nm using quartz cuvettes (10 mm path length) in a Shimadzu (Kyoto, Japan) UV-2401PC spectrophotometer. The Gt concentrations were obtained for each sample using a calibration curve obtained with Gt solutions between 2 μg/mL and 15 μg/mL.

Alternatively, 20 mg of Gt-Mnt-200 hybrid and 2 mL of PBS (phosphate buffer solution, pH 7) were added to plastic tubes wrapped in aluminum film, and kept in a shaking thermostatic bath at 37°C and 75 rpm. The tubes were removed from the bath at different time intervals and the suspension was filtered through a 0.45 μm pore size membrane (MF-Millipore Membrane Filter, 13 mm diameter) placed on a 13 mm diameter Swinnex® filter holder from Millipore (Burlington, Massachusetts, USA). The solid was air-dried at 40°C under dark conditions for 24 h, and then the remaining amount of antibiotic was determined by chemical analysis.

Antimicrobial Activity of the HPMC/gentamicin-montmorillonite Films

Study of the antimicrobial properties of the prepared films was done at the NanoBioMatters S.L., Paterna, Valencia (Spain) laboratories. Some pathogenic microorganisms present in hospital environments: *S. aureus* (CECT240, ATCC 6538P), *E. coli* (CECT 516, ATCC 8739), methicillin-resistant *S. aureus* (CECT 5190, ATCC 43300), *P. aeruginosa* (CECT 110, ATCC 10145), vancomycin-resistant *E. faecium* (CECT 5253), *A. baumannii* (CECT452, ACTT 15308), and *K. pneumoniae* (CECT 8453, ATCC 4352), were purchased from the Spanish Type Culture Collection (Valencia, Spain) and used to determine the antimicrobial activity of HPMC films with Gt-based clays. The strains were stored in Tryptone Soy Broth (TSB) with 20% glycerol at –80°C until needed. For experimental use, the stock cultures were maintained by regular subculture on Tryptic Soy Agar (TSA) slants at 4°C and transferred monthly. A loopful of each bacterium was placed in 10 mL of TSB and incubated at 37°C overnight. A 100 μL aliquot from each overnight culture was again transferred to TSB and grown at 37°C to the mid-exponential phase of growth. These cultures served as the inoculum in the susceptibility studies according to ASTM E2149, starting with ~10^5 CFU/mL in the test tubes. These CFU counts were obtained accurately and reproducibly by inoculation of 0.1 mL of the culture having an absorbance value of 0.2, as determined by optical density at 600 nm by means of UV-Vis spectroscopy.

The antimicrobial effectiveness of the films obtained was evaluated according to the standard ASTM E2149-01 (Standard test method for determining the antimicrobial activity of immobilized antimicrobial agents under dynamic contact conditions, 2001). For this method, 0.05 g of each film was introduced into test tubes each containing 5 mL of phosphate buffer solution. A sample with a film without clay was used as a control. Subsequently, each tube was inoculated with 10^5 cells/mL of *S. aureus* in mid-exponential phase and incubated in a wrist action shaker (160 rpm) at 25°C for 24 h. Bacterial counts were then enumerated by sub-cultivation on TSA plates. All samples were run in duplicate.

Furthermore, the modified disc-diffusion method (Bauer et al., 1966) was used to evaluate by visual inspection the antimicrobial activity of the films obtained against all the bacterial isolates. For this method, tryptic soy agar plates were seeded with 200 μL of bacterial inoculum (concentration 2.8–5.3×10^8 cells/mL). 6 mm diameter samples were placed on inoculated plates and then incubated at 37°C for 24 h. All samples were run in duplicate. An inhibition zone was monitored after incubation, and the presence of a bacterial growth inhibition halo around the samples was studied.

RESULTS AND DISCUSSION

Preparation of Gentamicin-montmorillonite Hybrids and Study of the Adsorption Isotherm

The amino groups of the sugar rings of Gt exhibit variable pKa values which range from 5.7 to 9.9 (Lesniak et al., 2003). Thus, Gt carries a net positive charge up to pH values of ~10 which makes possible its intercalation in Na^+-montmorillonite by means of cationic exchange processes. The adsorption isotherm at 294 K from Gt sulfate solutions on Na^+-montmorillonite (Fig. 2) shows the amount of Gt adsorbed, deduced from the CHN chemical analyses of the Gt-Mnt hybrids. In order to investigate the adsorption process, three models of equilibrium isotherms were applied, the Langmuir (Eq. 1), the Freundlich (Eq. 2), and the Redlich-Peterson (Eq. 3) isotherms:

$$q_e = \frac{q_m K_a C_e}{1 + K_a C_e}$$

where q_e is the equilibrium adsorption capacity (mg/g), C_e is the equilibrium liquid phase concentration (mg/L), q_m is the maximum adsorption capacity (mg/g), and K_a is adsorption equilibrium constant (L/mg).

$$q_e = K_F C_e^{1/n}$$

where C_e is the equilibrium concentration in the solution (mg/L), q_e is the equilibrium adsorption capacity (mg/g), and K_F and $1/n$ are empirical constants.

$$q_e = \frac{A C_e}{1 + B C_e^g}$$

where A, B, and g ($0 < g < 1$) are three constants of this model which combines both the Freundlich and Langmuir isotherms.

As shown in Table 3, the Langmuir and the Redlich-Peterson isotherms provided the best fit to the adsorption data of Gt on Na^+-montmorillonite at 294 K, indicating the homogeneity in the adsorption sites.

The Gibbs energy of adsorption, $\Delta G°$, calculated for these adsorption data was –18.6 kJ mol^{-1}, which is of the order of values obtained for adsorption of other antibiotics in clay minerals (Song et al., 2019). The negative value of Gibbs energy confirms the feasibility of the process and the

https://doi.org/10.1007/s42860-021-00156-3 Published online by Cambridge University Press

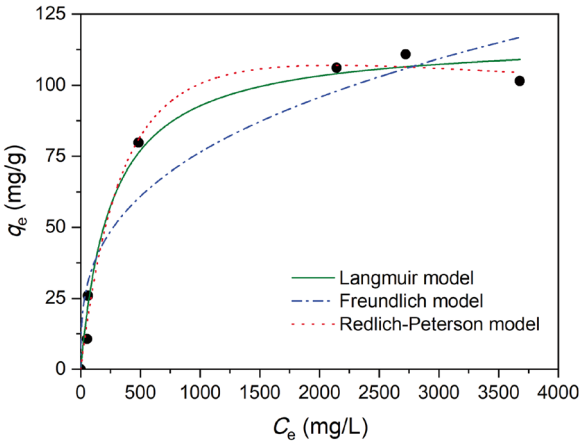

Fig. 2. Adsorption isotherm of Gt adsorption onto Na^+-montmorillonite obtained at 294 K. Amounts of Gt adsorbed were determined from CHN analysis

spontaneous nature of adsorption of Gt on Na^+-montmorillonite. The cationic exchange sites in the clay, with a CEC of 92.6 mEq/100 g, are assumed to be able to adsorb a certain amount of charged Gt due to protonation of $–NH_3^+$ and $–NH_2^+–$. The total charge depends on the protonation state of hydroxyl and amine groups at a given pH. In the present work, the pH value in the isotherm experiment was ~5.5. According to the study by Lesniak et al. (2003), the ionic forms of Gt at the experimental pH should be mainly Gt^{5+}, with a small amount of Gt^{4+}. As a result, the total amount of Gt that could be retained by the clay used in this study should be between 0.185 mmol/g and 0.232 mmol/g. The maximum amounts of adsorbed Gt according to the adsorption isotherm were ~0.22–0.24 mmol/g. Note, however, that these values were obtained for unwashed samples, where the amount adsorbed can exceed the CEC of the clay due to molecules adsorbed on the external surface. The chemical analysis of the Gt-Mnt-600 hybrid after washing gave a value of 0.183 mmol/g, which would correspond mainly to intercalated Gt and suggests that Gt^{5+} is the Gt species intercalated in the clay interlayer space.

Characterization of Gentamicin-montmorillonite Hybrids

The XRD patterns of the pristine clay and the Gt-montmorillonite nanohybrids (Fig. 3) confirm the intercalation of Gt in the clay interlayer space by the shift of the 001 reflection toward lower 2θ values as the Gt:clay ratio increased. As shown in XRD results, the d_{001} spacing reached 1.43 nm when the adsorption reached equilibrium, corresponding to an interlayer distance of 0.47 nm. The lower-energy configuration of Gt, with a two-dimensional size of a Gt molecule, was reported by Doadrio et al. (2004) to be 0.52 nm × 1.53 nm. For Gt-Mnt-500, Gt-Mnt-600, and Gt-Mnt-730 hybrid samples, the distance between two consecutive smectite layers was ~0.47 nm, similar to the size of a Gt molecule in one dimension. The result suggests that the Gt molecule is intercalated as a monolayer with the three rings of the Gt molecule positioned roughly parallel to the smectite layers. This finding is also in agreement with results and modeling of Gt adsorbed on bentonites reported by Iannuccelli et al. (2018).

In order to provide experimental confirmation of the optimal layer spacing, the FWHM profile as a function of d_{001} of Gt-Mnt samples was examined. Changes in FWHM have been attributed previously to the evolution of different configurations of the intercalated molecules, whereby, in a profile of FWHM values as a function of d_{001}, an increase in FWHM typically indicates interstratifications of different layer types. As reported previously (Aristilde et al., 2013), a minimum FWHM would be reached when the clay interlayers are saturated with adsorbed Gt, and the corresponding layer spacing would be considered optimal for the binding of Gt in the interlayer. With the increasing amount of Gt intercalated in the clay, the FWHM decreased from values of ~0.9°2θ for Mnt and Gt-Mnt-25 to values of ~0.5°2θ for the other hybrids with greater Gt loadings. Such a decrease in FWHM was proposed to be due to a gradual change in the interlayer configuration occurring homogeneously within all layers, wherein the molecules would change position or orientation, e.g. from being stretched to a relatively flat chain molecule with high energy to being a stable molecule chain which is less distorted.

Energy-dispersive X-ray analysis (EDX) measurements were performed on the starting montmorillonite, and on the nanohybrid samples labeled as Gt-Mnt-50, Gt-Mnt-200, and Gt-Mnt-730. The EDX results indicate a decreasing Na^+ ratio with the increasing amount of Gt adsorbed on the clay Wt(Na^+) (Fig. 3B). In this way, the predominance of ion-exchange mechanisms driving the intercalation of the Gt into the phyllosilicate substrate is confirmed experimentally.

The FTIR spectra were registered for Na^+-montmorillonite, the Gt-montmorillonite nanohybrid labeled as Gt-Mnt-730, and pristine Gt sulfate (Fig. 4). Beside the vibrational bands characteristic of the silicate, ν_{OH} of Al,Mg(OH) 3633 cm^{-1}; ν_{OH} of H_2O 3451 and 3249 cm^{-1}; δ_{HOH} 1637 cm^{-1}; and ν_{SiO} of Si–O–Si 1045 cm^{-1} (Fig. 4a), the bands attributed to the intercalated Gt are also observed in the spectrum of Gt-clay hybrid (Fig. 4b). The characteristic vibration bands of Gt in the hybrid material are observed at practically the same

Table 3. Isotherm parameters obtained using the non-linear Langmuir, Freundlich, and Redlich-Peterson equations for the adsorption data of Gt on Na^+-montmorillonite at 294 K

Isotherm model	Parameters	
Langmuir	q_m, (mg/g)	117 ± 5
	K_a, (L/mg)	0.0039 ± 0.0009
	r^2	0.983
Freundlich	n	3.1 ± 0.7
	K_F, (mg/g)(L/mg)$^{1/n}$	8.0 ± 4.8
	r^2	0.907
Redlich-Peterson	g	1.2 ± 0.1
	B, (L/mg)g	0.0006 ± 0.0008
	A, L/g	0.33 ± 0.08
	r^2	0.987

https://doi.org/10.1007/s42860-021-00156-3 Published online by Cambridge University Press

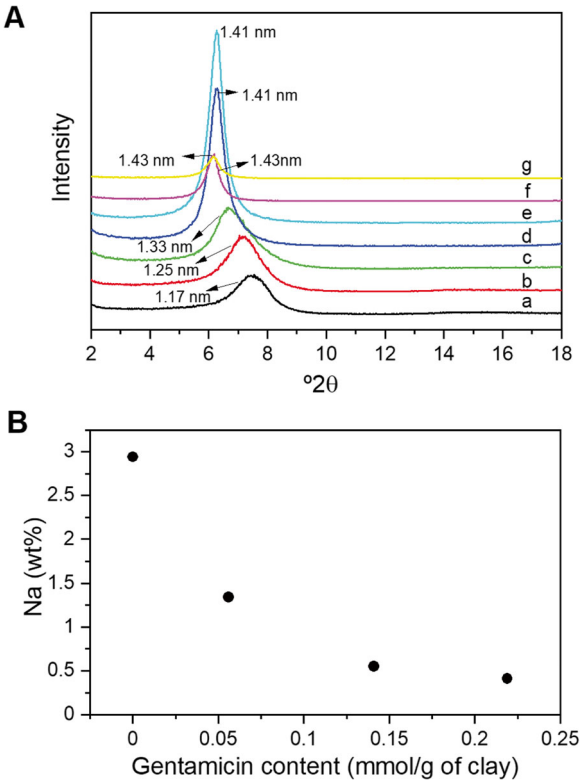

Fig. 3. **A** XRD patterns of (a) starting montmorillonite, and (b) Gt-Mnt-25, (c) Gt-Mnt-50, (d) Gt-Mnt-200, (e) Gt-Mnt-500, (f) Gt-Mnt-597, and (g) Gt-Mnt-730 Gt-montmorillonite nanohybrid samples obtained in the adsorption study. **B** Decrease of sodium content in the samples as Gt content increases in the hybrids, as determined by EDX in pristine Mnt and Gt-Mnt-50, Gt-Mnt-200, and Gt-Mnt-730 hybrid samples

wavenumbers as in the pristine Gt sulfate (Fig. 4c). This confirms that Gt is present as a protonated species in interaction with the silicate layers, which now act as counterions. Also, the N–H in-plane deformation vibration bands of amine groups of Gt appeared at a value very close to that of δ_{HOH} of the silicate, and a band due to the overlapping of those bands was observed at 1632 cm^{-1} in the spectrum of the Gt-Mnt hybrid, which suggests a possible intermolecular hydrogen bonding between water and Gt molecules in the interlayer region (Rapacz-Kmita et al., 2015). At ~1048 cm^{-1} in the spectrum of Gt-clay sample, the vibration band for C–O–C of Gt overlaps the band of Si–O–Si of the clay. The vibration band at 1531 cm^{-1} in the spectrum of Gt (Fig. 4c), which corresponds to the symmetric deformation vibration (δ_{NH3}^{+}) of the protonated primary amine group, shifted to 1529 cm^{-1} after Gt was intercalated in the clay.

According to the TG curves (Fig. 5), the mass loss due to water-molecule desorption takes place from 30–87°C and at 160°C for starting silicate and Gt-clay, respectively. This may be due to the interaction of the water molecules with intercalated Gt in the interlayer region, as suggested by FTIR data. Such mass loss was ~4.6% in the starting silicate, while the Gt-clay hybrid showed a slightly larger value of 5.4%, which may be due to the high water-retention capacity of Gt. The thermal decomposition process of Gt was similar in the hybrid material to what it was in the pristine compound, although the different decomposition steps are not as well defined in the intercalated material. The last mass loss ascribed to dehydroxylation of the clay started at a slightly lower temperature, ~500°C in the hybrid instead of 580°C in the pristine clay, partially overlapping the last decomposition phase of Gt. This effect is probably due to the different interlayer cation present in the hybrid.

The stability of Gt in the montmorillonite-based hybrids was evaluated using the Gt-Mnt-200 and Gt-Mnt-600 hybrid samples. The Gt-Mnt-600 sample contains 108.6 mg/g clay (0.234 mmol/g clay), i.e. with excess Gt probably adsorbed on the external surface of the clay. This sample was immersed in deionized water and, after given intervals, the values of Gt released were determined in the supernatant by UV spectrophotometry following reaction with phthaldialdehyde. The remaining amounts of Gt in the hybrid after various time intervals (Fig. 6) show that, after 24 h, ~15% of Gt was released, with ~0.198 mmol/g remaining in the hybrid. If the same study had been carried out with a sample previously washed to remove the excess adsorbed antibiotic, no Gt was detected in the supernatant by the phthaldialdehyde procedure after 24 h.

The stability of the Gt-Mnt hybrids was also evaluated in a buffered solution at pH 7 using the Gt-Mnt-200 hybrid sample, which contains 0.172 mmol of antibiotic per g of clay. As this value is less than the CEC of the clay, the antibiotic molecules are probably intercalated in the clay interlayer space with no excess Gt adsorbed on the external surface. The results of chemical analyses of the solids recovered at each studied time showed that large amounts of Gt were not released from the Gt-Mnt-200 hybrid under these experimental conditions (Fig. 6). The quantity of Gt adsorbed on the clay decreased slightly from the initial 0.172 mmol/g to 0.167 mmol/g after 24 h. At pH 7, Gt was protonated as a mixture of Gt^{3+}, Gt^{4+}, and Gt^{5+}, which causes Gt compounds to be retained in the interlayer of montmorillonite because of high electrostatic attraction; they cannot be replaced easily by sodium or any other ions present in the medium.

HPMC/gentamicin-montmorillonite Bionanocomposite Films

A set of HPMC/Gt-montmorillonite bionanocomposite films was prepared by dispersing appropriate amounts of the Gt-Mnt-500 hybrid sample, containing 106.1 mg/g of clay, in aliquots of HPMC aqueous solution, as detailed in the Experimental Section. The compositions of the bionanocomposite films prepared are summarized in Table 2. After drying, the films were separated from the molds as self-standing films showing a uniform aspect. The morphology of the Gt-Mnt-HPMC bionanocomposite films was analyzed by FE-SEM (Fig. 7). The surface aspect of the 0.5%Gt-Mnt-HPMC membrane (Fig. 7a) with a relatively small amount of hybrid (5.2%) shows a smooth aspect where some small dots, probably related to hybrid

https://doi.org/10.1007/s42860-021-00156-3 Published online by Cambridge University Press

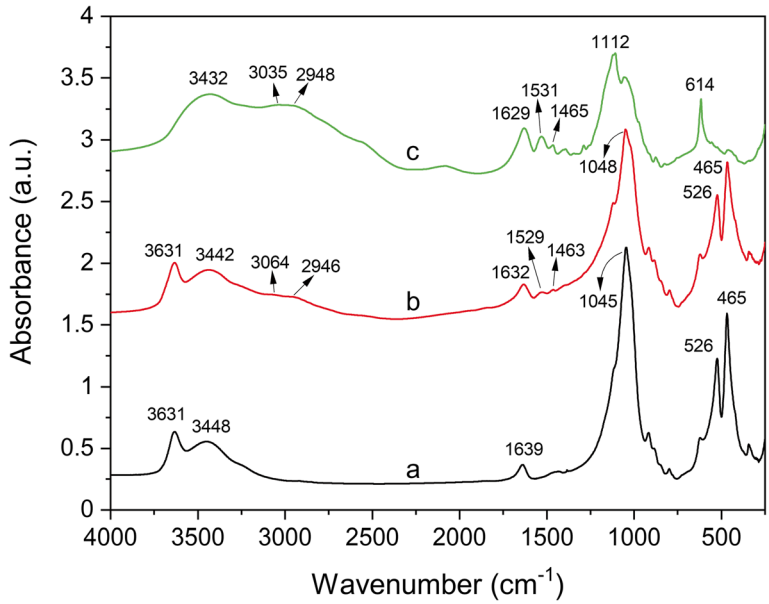

Fig. 4. IR spectra (4000–250 cm^{-1} region) of (a) the starting Na^{+}-montmorillonite, (b) the Gt-clay nanohybrid labeled as Gt-Mnt-730, and (c) starting Gt sulfate

particles which were embedded in the polymer located close to the surface. The presence of such spots was discerned more clearly when the hybrid content increased, as observed in the images of the 1.4%Gt-Mnt-HPMC membrane (Fig. 7b, c). In this case, the image at higher magnification (Fig. 7c) allowed observation of particles of the clay inserted in the polymer bulk. The cross-section image of this membrane (Fig. 7d) confirms the homogeneous distribution of the nanofiller on the polymer matrix which appeared as a continuous phase with a consistent texture.

The success of antibiotic-loaded films depends heavily on favorable mechanical properties. The pure HPMC film has an elastic modulus of 2.7 GPa and a percentage of elongation at break of ~17%, as determined from the corresponding stress-strain curves (Fig. S1, Supplementary Material). The effects of

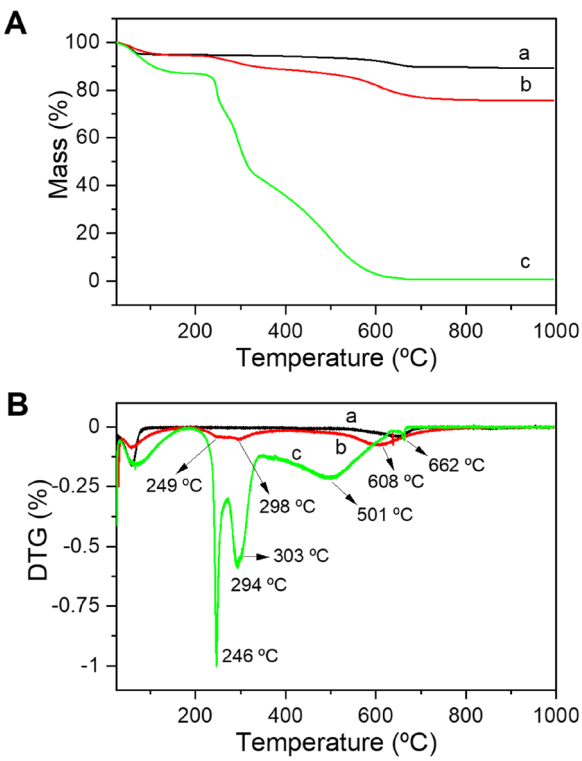

Fig. 5. **A** TG and **B** DTG curves in the 25–1000°C temperature range, obtained under air flow, of (a) Na^{+}-montmorillonite, (b) Gt-Mnt-730 hybrid sample, and (c) starting Gt sulfate

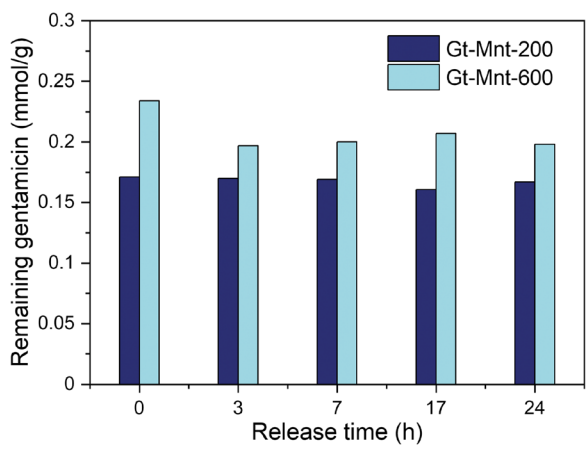

Fig. 6. Release profiles from Gt-Mnt-600 hybrid sample in deionized water and from Gt-Mnt-200 in 50 mM PBS (*p*H=7) at 37°C, showing the amount of Gt remaining adsorbed in each hybrid at different time intervals

https://doi.org/10.1007/s42860-021-00156-3 Published online by Cambridge University Press

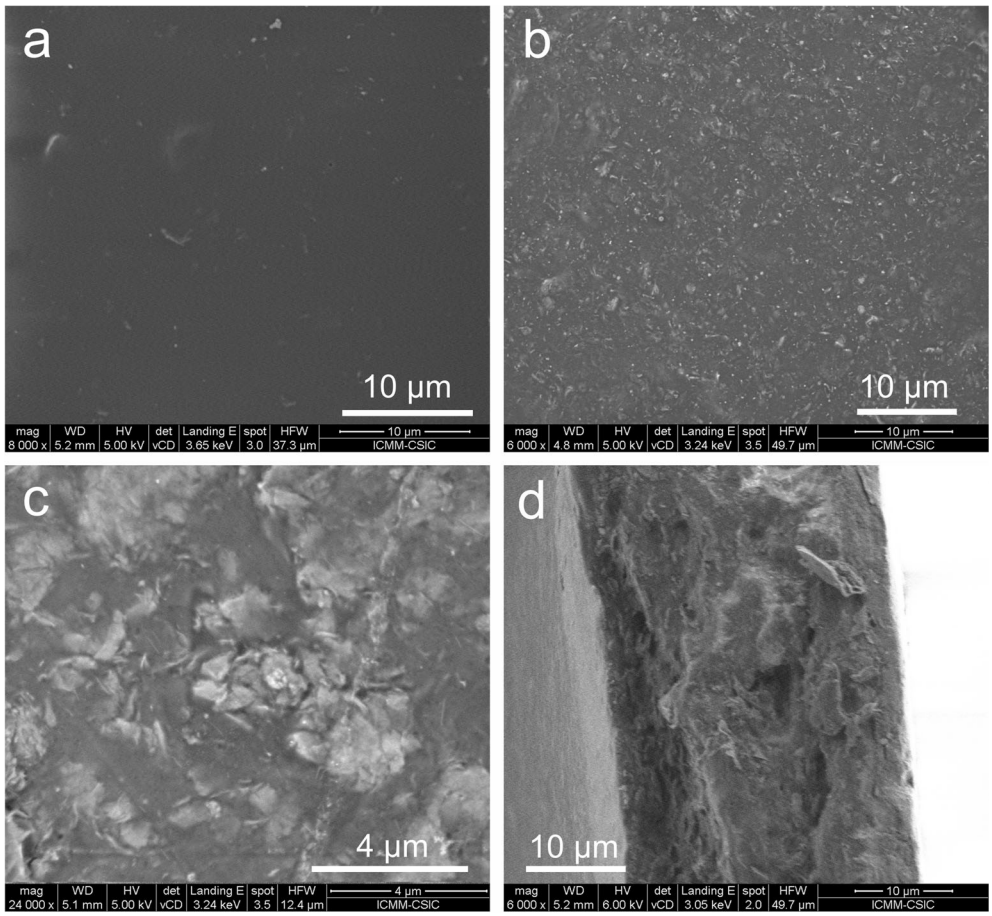

Fig. 7. FE-SEM images of the surface of **a** the 0.5%Gt-Mnt-HPMC film, **b** and **c** the 1.4%Gt-Mnt-HPMC film at different magnifications, and **d** cross-section of the 1.4%Gt-Mnt-HPMC film

increasing Gt-Mnt content on the elastic or Young's modulus and elongation at break values of the Gt-Mnt-HPMC films obtained are listed in Table 4. The incorporation of hybrid in the HPMC matrix produced an increase in the elastic modulus values with respect to that of pure HPMC film, indicating an increase in the films' stiffness. The increase in hybrid loading also gave rise to a decrease in the value of elongation at break, which is observed commonly in reinforced nanocomposites and is probably attributed to the reduction in mobility of the polysaccharide chains due to their interaction with the reinforcing agent.

The water-absorption tendency of the films containing different loadings of Gt-Mnt hybrid was studied in comparison to the pristine HPMC film. The water sorption isotherms (Fig. 8) show the weight increase due to water uptake expressed as grams of water incorporated per 100 g of dry sample as a function of the relative humidity (%). The adsorption-desorption isotherms of the bionanocomposite films show a very similar behavior, also close to that of the pristine HPMC, with just minor differences at relative humidity values of >80% where a slight reduction in water uptake was observed as the hybrid amount was increased. The

Table 4. Elastic modulus and percentage of elongation at break of HPMC bionanocomposite films at different loadings of the Gt-Mnt hybrid

Sample	Gt-Mnt content (%)	Elastic modulus (GPa)	Elongation at break (%)
HPMC	0	2. 7 ± 0.1	17 ± 6
0.26%Gt-Mnt-HPMC	2.7	3.08 ± 0.05	9 ± 2
0.5%Gt-Mnt-HPMC	5.2	3.26 ± 0.30	4.8 ± 0.9
1.4%Gt-Mnt-HPMC	14.2	4.10 ± 0.32	3.1 ± 0.4

https://doi.org/10.1007/s42860-021-00156-3 Published online by Cambridge University Press

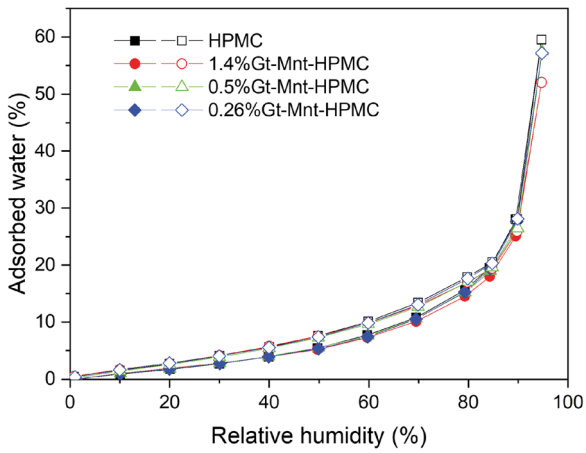

Fig. 8. Water sorption isotherms at 25°C of pristine HPMC film and Gt-Mnt-HPMC bionanocomposite films. Solid symbols: adsorption; hollow symbols: desorption

results confirmed that incorporation of Gt-Mnt hybrids does not reduce the hydrophilicity of HPMC, which is beneficial for wound-dressing applications (Jin et al., 2016).

The antimicrobial activity of the Gt-Mnt-HPMC bionanocomposite films was studied according to ASTM E2149. The HPMC-based films showed antimicrobial properties compared with the control tube with peptone water. The HPMC or/and the montmorillonite samples used in the present study, evaluated as controls, i.e. free of Gt, showed no detectable antimicrobial effect. The antimicrobial properties against *S. aureus* (CECT 240, ATCC 6538P) of the samples obtained are listed in Table 5. These samples presented maximum antimicrobial properties regardless of the amount of Gt within the film.

The antimicrobial properties of HPMC films labeled as 0.5%Gt-Mnt-HPMC, containing 4.7% of clay and 0.5% of Gt, were evaluated by visual inspection according to the modified disc diffusion method (Fig. 9). The HPMC film with modified clay was able to reduce completely microbial development around the sample for all of the microorganisms studied except for methicillin-resistant *S. aureus* (MRSA), where only a slight colony reduction was observed. Experiments carried out with HPMC films or Whatman filters loaded directly with Gt showed a clear inhibition zone in agar plates seeded with *E. coli* and *S. aureus* (Fig. S2, Supplementary Material). The control samples, without clay, were dissolved completely during the incubation process due to their low water resistance, but also because they could serve as nutrient media for the microbial growth. On the other hand, the film with Gt-modified clay does not allow microbial growth on itself and, consequently, it cannot be degraded by microorganisms. Moreover, the incorporation of clays within the polymer matrix could enhance the physical properties of the film, increasing their water resistance.

The antimicrobial properties of Gt incorporated in a biopolymer matrix for medical purposes have already been studied by several authors as described in the introduction section. The effectiveness of PHBV/Gt formulations for therapeutic modalities in implant-related staphylococcal infections was demonstrated by Rossi et al. (2004). A biodegradable PLA/PEG Gt delivery system that showed great potential for prophylaxis of post-operative infection was described by Huang and Chung (2001). Great antimicrobial properties in PLA composites with silver-organomodified clays were demonstrated by Busolo et al. (2010). The combination of antibiotic-modified clays with inorganic antimicrobials such as silver-modified clays could lead to additive or even synergistic biocide effects against a broad range of microorganisms. Consequently, the amount of antibiotic or antimicrobial agents required to achieve a satisfactory effect could decrease significantly. In fact, some recent works have addressed the use of clay-based systems in combination with biopolymers to produce effective bionanocomposites with a biocide effect (Aguzzi et al., 2014; Ambrogi et al., 2017; Rebitski et al., 2018; Lisuzzo et al., 2020). In particular, examples of Gt-clay bionanocomposites for uses in implants and scaffolds have been described (e.g. Kimna et al., 2019), though few approaches have been made in terms of systems for applications in wound- and burn-dressings tissues, where the bionanocomposite system reported here is very promising.

CONCLUSIONS

Amongst other antibiotics, Gt has been associated with clay minerals of diverse characteristics (e.g. smectites,

Table 5. Antimicrobial properties of the obtained films against *S. aureus* according to ASTM E2149

Sample description	CFU/mL	CFU/mL	Mean	% Bacterial reduction
Control without film	2.02E+07		2.02E+07	-
Control with HPMC film	1.92E+07	1.56E+07	1.74E+07	-
0.26%Gt-Mnt-HPMC	1.00E+00	1.00E+00	1.00E+00	100.00
0.5%Gt-Mnt-HPMC	1.00E+00	1.00E+00	1.00E+00	100.00
1.4%Gt-Mnt-HPMC	1.00E+00	1.00E+00	1.00E+00	100.00
2.1%Gt-Mnt-HPMC	1.00E+00	1.00E+00	1.00E+00	100.00
3.4%Gt-Mnt-HPMC	1.00E+00	1.00E+00	1.00E+00	100.00
6.0%Gt-Mnt-HPMC	1.00E+00	1.00E+00	1.00E+00	100.00

https://doi.org/10.1007/s42860-021-00156-3 Published online by Cambridge University Press

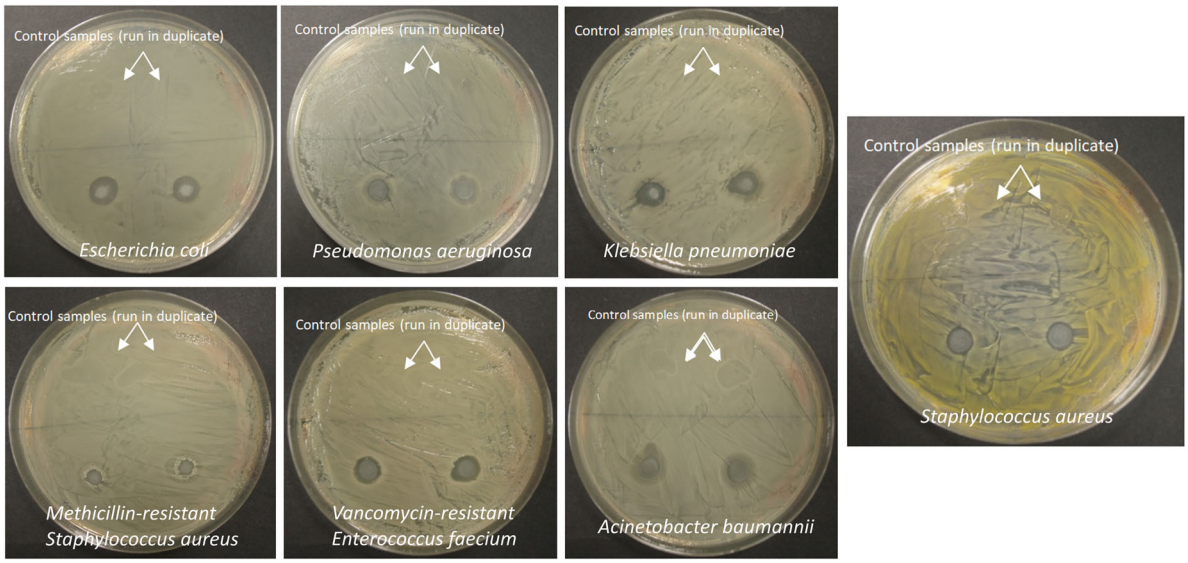

Fig. 9. Inhibition halo around the 0.5%Gt-Mnt-HPMC film samples after incubation against different microorganisms: *E. coli*, *P. aeruginosa*, *S. aureus*, methicillin-resistant *S. aureus,* vancomycin-resistant *E. faecium, A. baumannii* and *K. pneumoniae*

kaolinite, halloysite) to produce, alone or in combination with polymers, bioactive systems designed mainly for use in implants and scaffolds in bone-regeneration and tissue-engineering applications. In the present study, Gt was adsorbed to montmorillonite (Cloisite®-Na+) by means of an ion-exchange mechanism, being arranged as a monolayer of Gt^{5+} cations compensating the negative charge of the silicate layers. The interaction of the Gt ions with the silicate is strong enough to provide a stable hybrid material, where the release in water and buffer media is slowed. This is promising in terms of the development of a sustained-delivery system. Intercalation compounds with a tuned amount of the drug were later assembled to HPMC at different loadings. These bionanocomposites can be processed easily as films offering better mechanical resistance than the pristine biopolymer, although the elasticity decreases with the hybrid loading. The presence of the hybrids does not reduce the hydrophilic character of HPMC showing similar water sorption isotherms. Besides, the presence of the clay reduces the swelling ability of HPMC films, avoiding their disintegration. Antimicrobial, in vitro tests for *Staphylococcus aureus* (ASTM E2149) show a maximum efficacy even for small Gt contents, proving interest in applications as a healing-wound tissue. Such significant antibacterial activity with small Gt contents is advantageous because low hybrid loadings in the HPMC films contribute to the preservation of the elasticity of the films. The bacterial reduction was also confirmed in agar plates with other microorganisms (*E. coli, P. aeruginosa, S. aureus,* methicillin-resistant *S. aureus* (MRSA), vancomycin-resistant *E. faecium, A. baumannii*, and *K. pneumonia*), showing, in all cases, an inhibition halo except for the case of MRSA, where the inhibitory effect is only partial. These bionanocomposite films show promising properties for application as wound dressings.

SUPPLEMENTARY INFORMATION

The online version contains supplementary material available at https://doi.org/10.1007/s42860-021-00156-3.

ACKNOWLEDGMENTS

Financial support from CICYT (project MAT2012-31759) and AEI (project PID2019-105479RB-I00) is acknowledged. The authors thank Patricia Fernández-Saiz and Mercedes Monte-Serrano from NanoBioMatters S.L., Paterna, Valencia (Spain), for carrying out the antimicrobial activity study.

Funding

Open Access funding provided thanks to the CRUE-CSIC agreement with Springer Nature. Funding sources are as stated in the Acknowledgments.

Compliance with Ethical Statements

Conflict of Interest

The authors declare that they have no conflict of interest.

REFERENCES

Aguzzi, C., Sandri, G., Bonferoni, C., Cerezo, P., Rossi, S., Ferrari, F., & Viseras, C. (2014). Solid state characterisation of silver sulfadiazine loaded on montmorillonite/chitosan nanocomposite for wound healing. *Colloids and Surfaces B: Biointerfaces, 113*, 152–157.

Allègre, J. (2012). Les silicates d'alumine (argiles) en therapeutique. Une pratique coutumière ancienne relayée dans la médecine moderne. PhD Thesis. Université Paris XIII, France.

Ambrogi, V., Pietrella, D., Nocchetti, M., Casagrande, S., Moretti, V., De Marco, S., & Ricci, M. (2017). Montmorillonite–chitosan–chlorhexidine composite films with antibiofilm activity and improved cytotoxicity for wound dressing. *Journal of Colloid and Interface Science, 491*, 265–272.

Aristilde, L., Lanson, B., & Charlet, L. (2013). Interstratification patterns from the ph-dependent intercalation of a tetracycline antibiotic within montmorillonite layers. *Langmuir, 29*, 4492–4501. https://doi.org/10.1021/la400598x

Aviv, M., Berdicevsky, I., & Zilberman, M. (2007). Gentamicin-loaded bioresorbable films for prevention of bacterial infections associated with orthopedic implants. *Journal of Biomedical Materials Research. Part A, 83*, 10–19. https://doi.org/10.1002/jbm.a.31184

Bauer, A. W., Kirby, W. M. M., Sherris, J. C., & Turck, M. (1966). Antibiotic susceptibility testing by a standardized single disk method. *American Journal of Clinical Pathology, 45*, 493–496.

Busolo, M. A., Fernandez, P., Ocio, M. J., & Lagaron, J. M. (2010). Novel silver-based nanoclay as an antimicrobial in polylactic acid food packaging coatings. *Food Additives & Contaminants. Part A, Chemistry, Analysis, Control, Exposure & Risk Assessment, 27*, 1617–1626. https://doi.org/10.1080/19440049.2010.506601

Butko, P., Salamon, Z., & Tien, H. T. (1990). Adsorption of gentamicin onto a bilayer lipid membrane. *Bioelectrochemistry and Bioenergetics, 23*, 153–160. https://doi.org/10.1016/0302-4598(90)85004-2

Carja, G., Niiyama, H., Ciobanu, G., & Aida, T. (2007). Towards new drugs formulations: Gentamicin–anionic clay as nanohybrids. *Materials Science and Engineering: C, 27*, 1129–1132. https://doi.org/10.1016/j.msec.2006.07.017

Castro-Smirnov, F. A., Pietrement, O., Aranda, P., Bertrand, J. R., Ayache, J., Le Cam, E., Ruiz-Hitzky, E., & Lopez, B. S. (2016). Physical interactions between DNA and sepiolite nanofibers, and potential application for DNA transfer into mammalian cells. *Scientific Reports, 6*, 36341. https://doi.org/10.1038/srep36341

Castro-Smirnov, F. A., Ayache, J., Bertrand, J. R., Dardillac, E., Le Cam, E., Pietrement, O., Aranda, P., Ruiz-Hitzky, E., & Lopez, B. S. (2017). Cellular uptake pathways of sepiolite nanofibers and DNA transfection improvement. *Scientific Reports, 7*, 5586. https://doi.org/10.1038/s41598-017-05839-3

Choy, J. H., Kwak, S. Y., Jeong, Y. J., & Park, J. S. (2000). Inorganic layered double hydroxides as nonviral vectors. *Angewandte Chemie International Edition, 39*, 4042–4045.

Colombo, P. (1993). Swelling-controlled release in hydrogel matrices for oral route. *Advanced Drug Delivery Reviews, 11*, 37–57. https://doi.org/10.1016/0169-409X(93)90026-Z

Doadrio, A. L., Sousa, E. M. B., Doadrio, J. C., Pérez Pariente, J., Izquierdo-Barba, I., & Vallet-Regí, M. (2004). Mesoporous SBA-15 HPLC evaluation for controlled gentamicin drug delivery. *Journal of Controlled Release, 97*, 125–132. https://doi.org/10.1016/j.jconrel.2004.03.005

Elsner, J. J., Egozi, D., Ullmann, Y., Berdicevsky, I., Shefy-Peleg, A., & Zilberman, M. (2011). Novel biodegradable composite wound dressings with controlled release of antibiotics: Results in a guinea pig burn model. *Burns, 37*, 896–904. https://doi.org/10.1016/j.burns.2011.02.010

Faustini, M., Nicole, L., Ruiz-Hitzky, E., & Sanchez, C. (2018). History of organic–inorganic hybrid materials: Prehistory, art, science, and advanced applications. *Advanced Functional Materials, 28*, 1704158. https://doi.org/10.1002/adfm.201704158

Finkelman, R. B. (2019). The influence of clays on human health: a medical geology perspective. *Clays and Clay Minerals, 67*, 1–6. https://doi.org/10.1007/s42860-018-0001-9

Huang, Y. Y., & Chung, T. W. (2001). Microencapsulation of gentamicin in biodegradable PLA and/or PLA/PEG copolymer. *Journal of Microencapsulation, 18*, 457–465.

Hui, L. C., Malek, N. A. N. N., Awanluddin, M. Z., Asraf, M. H., Ishak, S. N., & Hadi, A. A. (2019). Adsorption of gentamicin on surfactant-kaolinite and its antibacterial activity. *Malasyam Journal of Fundamental and Applied Sciences, 15*, 686–689.

Iannuccelli, V., Maretti, E., Bellini, A., Malferrari, D., Ori, G., Montorsi, M., Bondi, M., Truzzi, E., & Leo, E. (2018). Organo-modified bentonite for gentamicin topical application: Interlayer structure and in vivo skin permeation. *Applied Clay Science, 158*, 158–168. https://doi.org/10.1016/j.clay.2018.03.029

Jeong, S. J., Kim, J.-H., Jung, D. H., Lee, K. H., Park, S. Y., Song, Y., Kang, I.-M., & Song, Y. G. (2018). Gentamicin-intercalated smectite as a new therapeutic option for Helicobacter pylori eradication. *Journal of Antimicrobial Chemotherapy, 73*, 1324–1329. https://doi.org/10.1093/jac/dky011.

Jin, S. G., Yousaf, A. M., Kim, K. S., Kim, D. W., Kim, D. S., Kim, J. K., Yong, C. S., Youn, Y. S., Kim, J. O., & Choi, H.-G. (2016). Influence of hydrophilic polymers on functional properties and wound healing efficacy of hydrocolloid based wound dressings. *International Journal of Pharmaceutics, 501*, 160–166. https://doi.org/10.1016/j.ijpharm.2016.01.044

Kim, M. H., Choi, G., Elzatahry, A., Vinu, A., Choy, Y. B., & Choy, J. H. (2016). Review of clay-drug hybrid materials for biomedical applications: administration routes. *Clays and Clay Minerals, 64*, 115–130. https://doi.org/10.1346/ccmn.2016.0640204

Kimna, C., Deger, S., Tamburaci, S., & Tihminlioglu, F. (2019). Chitosan/montmorillonite composite nanospheres for sustained antibiotic delivery at post-implantation bone infection treatment. *Biomedical Materials (Bristol, England), 14*, 44101. https://doi.org/10.1088/1748-605X/ab1a04

Lesniak, W., Mc Laren, J., Harris, W. R., Pecoraro, V. L., & Schacht, J. (2003). An isocratic separation of underivatized gentamicin components, H-1 NMR assignment and protonation pattern. *Carbohydrate Research, 338*, 2853–2862. https://doi.org/10.1016/j.carres.2003.08.005

Lisuzzo, L., Wicklein, B., Lo Dico, G., Lazzara, G., del Real, G., Aranda, P., & Ruiz-Hitzky, E. (2020). Functional biohybrid materials based on halloysite, sepiolite and cellulose nanofibers for health applications. *Dalton Transactions, 49*, 3830–3840. https://doi.org/10.1039/C9DT03804C

Luo, Y., & Mills, D. K. (2019). The effect of halloysite addition on the material properties of chitosan–halloysite hydrogel composites. *Gels, 5*, 40. https://doi.org/10.3390/gels5030040

MacNeil, J. D. & Cuerpo, L. (1995). Gentamicin. Residues of some veterinary drugs in animals and foods. FAO Food and Nutrition Paper 41/7. Food and Agriculture Organization, Rome, pp. 45–55.

Min, J., Braatz, R. D., & Hammond, P. T. (2014). Tunable staged release of therapeutics from layer-by-layer coatings with clay interlayer barrier. *Biomaterials, 35*, 2507–2517. https://doi.org/10.1016/j.biomaterials.2013.12.009

Moulds, R. F. W., & Jeyasingham, M. S. (2010). Gentamicin: a great way to start. *Australian Prescriber, 33*, 35–37. https://doi.org/10.18773/austprescr.2010.062

Murphy, K. D., Lee, J. O., & Herndon, D. N. (2003). Current pharmacotherapy for the treatment of severe burns. *Expert Opinion on Pharmacotherapy, 4*, 369–384. https://doi.org/10.1517/14656566.4.3.369

Oh, J.-M., Park, D.-H., Choi, S.-J., & Choy, J.-H. (2012). LDH Nanocontainers as bio-reservoirs and drug delivery carriers. *Recent Patents on Nanotechnology, 6*, 200–217. https://doi.org/10.2174/187221012803531538

https://doi.org/10.1007/s42860-021-00156-3 Published online by Cambridge University Press

Park, J. K., Choy, Y. B., Oh, J.-M., Kim, J. Y., Hwang, S.-J., & Choy, J.-H. (2008). Controlled release of donepezil intercalated in smectite clays. *International Journal of Pharmaceutics, 359*, 198–204. https://doi.org/10.1016/j.ijpharm.2008.04.012

Pavlukhina, S., Zhuk, I., Mentbayeva, A., Rautenberg, E., Chang, W., Yu, X., van de Belt-Gritter, B., Busscher, H. J., van der Mei, H. C., & Sukhishvili, S. A. (2014). Small-molecule-hosting nanocomposite films with multiple bacteria-triggered responses. *NPG Asia Materials, 6*, e121–e121. https://doi.org/10.1038/am.2014.63

Pierchala, M. K., Makaremi, M., Tan, H. L., Janarthanan, P., Muniyandy, S., Solouk, A., Lee, S. M., & Pasbakhsh, P. (2018). Nanotubes in nanofibers: Antibacterial multilayered polylactic acid/halloysite/gentamicin membranes for bone regeneration application. *Applied Clay Science, 160*, 95–105. https://doi.org/10.1016/j.clay.2017.12.016

Rapacz-Kmita, A., Stodolak-Zych, E. W. A., Ziabka, M., Rozycka, A., & Dudek, M. (2015). Instrumental characterization of the smectite clay–gentamicin hybrids. *Bulletin of Materials Science, 38*, 1069–1078. https://doi.org/10.1007/s12034-015-0943-7

Rapacz-Kmita, A., Bućko, M. M., Stodolak-Zych, E., Mikołajczyk, M., Dudek, P., & Trybus, M. (2017a). Characterisation, in vitro release study, and antibacterial activity of montmorillonite-gentamicin complex material. *Materials Science and Engineering: C, 70*, 471–478. https://doi.org/10.1016/j.msec.2016.09.031

Rapacz-Kmita, A., Stodolak-Zych, E., Dudek, M., Gajek, M., & Ziąbka, M. (2017b). Magnesium aluminium silicate–gentamicin complex for drug delivery systems. *Journal of Thermal Analysis and Calorimetry, 127*, 871–880. https://doi.org/10.1007/s10973-016-5918-4

Rapacz-Kmita, A., Foster, K., Mikołajczyk, M., Gajek, M., Stodolak-Zych, E., & Dudek, M. (2019). Functionalized halloysite nanotubes as a novel efficient carrier for gentamicin. *Materials Letters, 243*, 13–16. https://doi.org/10.1016/j.matlet.2019.02.015

Rapacz-Kmita, A., Szaraniec, B., MikoŁajczyk, M., Stodolak-Zych, E., Dzierzkowska, E., Gajek, M., & Dudek, P. (2020). Multifunctional biodegradable polymer/clay nanocomposites with antibacterial properties in drug delivery systems. *Acta of Bioengineering and Biomechanics, 22*, 83–92.

Rautureau, M., Figueiredo Gomes, C. d. S., Liewig, N., & Katouzian-Safadi, M. (2017). *Clays and Health. Properties and Therapeutic Uses*. Springer International Publishing.

Rebitski, E. P., Alcântara, A. C. S., Darder, M., Cansian, R. L., Gómez-Hortigüela, L., & Pergher, S. B. C. (2018). Functional carboxymethylcellulose/zein bionanocomposite films based on neomycin supported on sepiolite or montmorillonite clays. *ACS Omega, 3*, 13538–13550. https://doi.org/10.1021/acsomega.8b01026

Rebitski, E. P., Darder, M., Carraro, R., Aranda, P., & Ruiz-Hitzky, E. (2020). Chitosan and pectin core–shell beads encapsulating metformin–clay intercalation compounds for controlled delivery. *New Journal of Chemistry, 44*, 10102–10110. https://doi.org/10.1039/C9NJ06433H

Reshmi, C. R., Sundaran, S. P., Subija, T., & Athiyanathil, S. (2018). "Nano in micro" architecture composite membranes for controlled drug delivery. *Applied Clay Science, 166*, 262–275. https://doi.org/10.1016/j.clay.2018.08.015

Ribeiro, L. N. M., Alcântara, A. C. S., Darder, M., Aranda, P., Araújo-Moreira, F. M., & Ruiz-Hitzky, E. (2014). Pectin-coated chitosan-LDH bionanocomposite beads as potential systems for colon-targeted drug delivery. *International Journal of Pharmaceutics, 463*. https://doi.org/10.1016/j.ijpharm.2013.12.035

Rossi, S., Azghani, A. O., & Omri, A. (2004). Antimicrobial efficacy of a new antibiotic-loaded poly(hydroxybutyric-co-hydroxyvaleric acid) controlled release system. *Journal of Antimicrobial Chemotherapy, 54*, 1013–1018. https://doi.org/10.1093/jac/dkh477

Ruiz-Hitzky, E., Darder, M., Aranda, P., Martín del Burgo, M. A., & del Real, G. (2009). Bionanocomposites as new carriers for influenza vaccines. *Advanced Materials, 21*, 4167–4171. https://doi.org/10.1002/adma.200900181

Ruiz-Hitzky, E., Darder, M., Wicklein, B., Castro-Smirnov, F. A., & Aranda, P. (2019). Clay-based biohybrid materials for biomedical and pharmaceutical applications. *Clays and Clay Minerals, 67*, 44–58. https://doi.org/10.1007/s42860-019-0005-0

Sirousazar, M. (2013). Mechanism of gentamicin sulphate release in nanocomposite hydrogel drug delivery systems. *Journal of Drug Delivery Science and Technology, 23*, 619–621. https://doi.org/10.1016/S1773-2247(13)50094-3

Song, Y., Sackey, E. A., Wang, H., & Wang, H. (2019). Adsorption of oxytetracycline on kaolinite. *PLoS ONE, 14*, e0225335. https://doi.org/10.1371/journal.pone.0225335

Stavitskaya, A., Batasheva, S., Vinokurov, V., Fakhrullina, G., Sangarov, V., Lvov, Y., & Fakhrullin, R. (2019). Antimicrobial applications of clay nanotube-based composites. *Nanomaterials, 9*, 708 (20 p). https://doi.org/10.3390/nano9050708

Viseras, C., Cerezo, P., Sanchez, R., Salcedo, I., & Aguzzi, C. (2010). Current challenges in clay minerals for drug delivery. *Applied Clay Science, 48*, 291–295. https://doi.org/10.1016/j.clay.2010.01.007

Viseras, C., Carazo, E., Borrego-Sánchez, A., García-Villén, F., Sánchez-Espejo, R., Cerezo, P., & Aguzzi, C. (2019). Clay minerals in skin drug delivery. *Clays and Clay Minerals, 67*, 59–71. https://doi.org/10.1007/s42860-018-0003-7

Wang, B., Liu, H., Sun, L., Jin, Y., Ding, X., Li, L., Ji, J., & Chen, H. (2018). Construction of high drug loading and enzymatic degradable multilayer films for self-defense drug release and long-term biofilm inhibition. *Biomacromolecules, 19*, 85–93. https://doi.org/10.1021/acs.biomac.7b01268

Wei, W., Abdullayev, E., Hollister, A., Mills, D., & Lvov, Y. M. (2012). Clay nanotube/poly(methyl methacrylate) bone cement composites with sustained antibiotic release. *Macromolecular Materials and Engineering, 297*, 645–653. https://doi.org/10.1002/mame.201100309

Wicklein, B., Martín del Burgo, M. Á., Yuste, M., Darder, M., Llavata, C. E., Aranda, P., Ortin, J., del Real, G., & Ruiz-Hitzky, E. (2012). Lipid-based bio-nanohybrids for functional stabilisation of influenza vaccines. *European Journal of Inorganic Chemistry*, 5186–5191. https://doi.org/10.1002/ejic.201200579

Wicklein, B., Darder, M., Aranda, P., Martín del Burgo, M. A., del Real, G., Esteban, M., & Ruiz-Hitzky, E. (2016). Clay-lipid nanohybrids: Towards influenza vaccines and beyond. *Clay Minerals, 51*, 529–538. https://doi.org/10.1180/claymin.2016.051.4.01

Williams, L. B. (2017). Geomimicry: harnessing the antibacterial action of clays. *Clay Minerals, 52*, 1–24. https://doi.org/10.1180/claymin.2017.052.1.01

Williams, L. B. (2019). Natural antibacterial clays: historical uses and modern advances. *Clays and Clay Minerals, 67*, 7–24. https://doi.org/10.1007/s42860-018-0002-8

Williams, L. B., & Haydel, S. E. (2010). Evaluation of the medicinal use of clay minerals as antibacterial agents. *International Geology Review, 52*, 745–770. https://doi.org/10.1080/00206811003679737

Xu, Q., Li, X., Jin, Y., Sun, L., Ding, X., Liang, L., Wang, L., Nan, K., Ji, J., Chen, H., & Wang, B. (2017). Bacterial self-defense antibiotics release from organic–inorganic hybrid multilayer films for long-term anti-adhesion and biofilm inhibition properties. *Nanoscale, 9*, 19245–19254. https://doi.org/10.1039/C7NR07106J

Yang, J.-H., Lee, J.-H., Ryu, H.-J., Elzatahry, A. A., Alothman, Z. A., & Choy, J.-H. (2016). Drug–clay nanohybrids as sustained delivery systems. *Applied Clay Science, 130*, 20–32. https://doi.org/10.1016/j.clay.2016.01.021.

(Received 5 May 2021; revised 30 August 2021; AE: Youjun Deng)